First-principles study of the effect of vacancies on magnetic properties of $Zn_{1-x}Co_xO$ thin films

2010 J. Phys.: Condens. Matter 22 076002

(http://iopscience.iop.org/0953-8984/22/7/076002)

J. Phys.: Condens. Matter **22** (2010) 076002 (7pp) doi:10.1088/0953-8984/22/7/076002

First-principles study of the effect of vacancies on magnetic properties of $Zn_{1-x}Co_xO$ thin films

Qian Wang[1], Qiang Sun[2,3] and Puru Jena[1]

[1] Department of Physics, Virginia Commonwealth University, Richmond, VA 23284, USA
[2] Department of Advanced Materials and Nanotechnology, Peking University, Beijing, People's Republic of China
[3] Center for Applied Physics and Technology, Peking University, Beijing 100871, People's Republic of China

E-mail: qwang@vcu.edu

Received 25 September 2009, in final form 30 November 2009
Published 29 January 2010
Online at stacks.iop.org/JPhysCM/22/076002

Abstract

Due to the high solubility of Co in ZnO, the magnetic properties of Co-doped ZnO thin films have been extensively studied experimentally. Unfortunately, these results have led to diverse conclusions. To better understand the origin of the controversial experimental findings, we have carried out detailed theoretical studies, focusing on the role of concentration and distribution of Zn and O vacancies on the magnetism of $Zn_{1-x}Co_xO$ thin films. We find that when Co atoms are substitutionally doped in ZnO thin films without any defects, the magnetic coupling between Co atoms is intrinsically antiferromagnetic. The coupling, however, changes to ferromagnetic when sufficient oxygen vacancies are introduced. On the other hand, Zn vacancies stabilize the antiferromagnetic coupling, in sharp contrast to that found in $Zn_{1-x}Mn_xO$ thin films. Our theoretical studies explain the origin of the different magnetic behavior observed experimentally.

(Some figures in this article are in colour only in the electronic version)

1. Introduction

The study of dilute magnetic semiconductors (DMSs) has been a topic of great interest in the past decade since both charge and spin of electrons can be used for novel spintronic devices. DMSs are formed by replacing several atomic per cent of cations in a nonmagnetic semiconductor by magnetic transition metal (TM) ions and, therefore, they possess charge and spin degrees of freedom in a single material. Following the prediction by Dietl *et al* [1] that Mn-doped ZnO could have a large Curie temperature, numerous experiments have been carried out to search for TM-doped ZnO DMS materials that can be ferromagnetic (FM) at room temperature. Since II–VI type materials are known to support a greater concentration of dopants than III–V materials, ZnO is a material of choice. In addition, ZnO is a wide-band-gap semiconductor with novel magnetic, piezoelectric, electro-optic and electromechanical properties. Thus, ferromagnetism induced by TM doping can render ZnO with multi-functional characteristics.

One of the systems that have received a lot of attention in recent years involves Co-doped ZnO [2–22]. The structures of Co and ZnO are isomorphous. Since the atomic size of Co^{2+} and Zn^{2+} is similar, Co is highly soluble in ZnO [2]. Following the initial experimental report [3] that Co-doped ZnO thin films exhibit FM behavior with a Curie temperature (T_C) higher than room temperature, a number of studies of Co-doped ZnO thin films have been carried out. While some of these studies reveal ferromagnetism with a T_C above or close to room temperature (RT) [4–7], other studies found not only a low magnetic ordering temperature [8], but also the absence of ferromagnetism [9–11], and the presence of paramagnetism [12, 13] or antiferromagnetism [14–16] in this material. These controversial results give an indication that ferromagnetism in Co-doped ZnO is very sensitive to the experimental method and preparation conditions. Thus a question is raised: whether the FM order is intrinsic in the Co-substituted ZnO system or due to some external factors, such

as magnetic impurity clusters, metallic phase, or the presence of defects.

Recently, the role of defects in mediating ferromagnetism in $Zn_{1-x}Co_xO$ has been explored in experiments [17–22]. Zn interstitials (Zn_i) [17–19] as well as oxygen vacancies (V_O) [20–22] have been proposed to be responsible for room temperature ferromagnetism in this material. Theoretical studies of the effect of native point defects in pure bulk ZnO [23, 24] and in thin films [25] have been performed. However, theoretical data demonstrating ferromagnetism in TM-doped ZnO is very limited and conflicting. For example, Lee and Chang [26] studied the magnetic interaction in *bulk* $Zn_{1-x}Co_xO$ using the local-spin-density approximation and found that a sufficient supply of electron carriers is required to achieve ferromagnetism, while Spaldin [27], using the density functional theory approach based on pseudopotentials with localized atomic-orbital basis sets, suggested that ferromagnetism in Co- or Mn-doped *bulk* ZnO only occurs in the presence of simultaneous p-type doping (holes).

In this study, we present a first-principles study that addresses the following issues: (1) Whether the FM ordering is intrinsic in Co-substituted ZnO thin films or due to some external factors? (2) Does Co distribute uniformly as Mn does in ZnO thin films? Is there a fundamental difference between the magnetic properties of (Zn, Co)O and (Zn, Mn)O? (3) What is the mechanism for driving the magnetic coupling between Co atoms in ZnO thin films? If vacancies indeed play a role in mediating ferromagnetism, are they Zn and/or O vacancies? (4) What role do the concentration and distribution of vacancies play on the magnetic coupling?

2. Theoretical method

The ZnO thin film was modeled by a (1 × 2) 9-layer slab supercell having a wurtzite structure along the [11$\bar{2}$0] surface direction resulting in 36 formula units of ZnO. A vacuum region of 10 Å separated the slabs from one another along the [11$\bar{2}$0] direction. The central three layers are kept frozen in their bulk positions, while the atoms in the top and bottom three layers of the slab were allowed to relax without any symmetry constraint. The surface layers of the top and bottom sides of the slab were taken to be identical, which makes the thin film supercell centro-symmetric. The slab extends to infinity along the [0001] and [1$\bar{1}$00] directions through the periodic repetition of the supercell to mimic the real thin film surface situation. To study the magnetic coupling between Co atoms and the distribution of Co atoms in ZnO thin films, we have replaced two Zn atoms with two Co atoms at different sites, corresponding to a doping concentration of 11.11%. Six different configurations corresponding to Co-substitution, as shown in figure 1, were studied. The calculations of total energies, forces and optimization of geometries were carried out using spin polarized density functional theory (DFT). The PW91 functional [28] for the generalized gradient approximation (GGA) for exchange and correlation potential was used. A plane wave basis set and the projector augmented wave (PAW) potentials [29] with the valence states $3d^{10}$ and $4s^2$ for Zn; $3d^7$ and $4s^2$ for Co; $2s^2$ and $2p^4$ for O, as implemented in the *Vienna Ab initio Simulation Package* (VASP) [30] was employed. The energy cutoff in all these calculations was set to 350 eV (the default of maximum cutoff energy is 276.995 eV). The convergence in energy and force were set to 10^{-4} eV and 10^{-3} eV $Å^{-1}$, respectively.

In order to study the effect of Co concentration on the magnetic coupling and defect distribution in the thin film, we generated a (2 × 2) 7-layer slab supercell having the same [11$\bar{2}$0] surface direction, and containing a total of 112 atoms ($Zn_{56}O_{56}$). For the (1 × 2) 9-layer slab supercell, we used (6 × 4 × 1) and (8 × 6 × 1) Monkhorst–Pack grids [31], respectively, for the structure optimization and for total energy and charge density calculations. For the (2 × 2) 7-layer supercell, (5 × 5 × 1) and (7 × 7 × 1) k-point meshes are selected. In all the calculations, the atomic coordinates of all the atoms (except for those in the central layers which were fixed in their bulk positions) were relaxed without any symmetry constraint. It was verified that the thickness of the slab and the vacuum space are adequate to study the effects of the surface [32]. The binding energy and the Z–O bond lengths were found to converge in the 7-layer slab. The [11$\bar{2}$0] surface reconstruction and the reliability of our calculations have been well established from our previous work [25, 32, 35]. For the dimers of Co_2, the calculated ground state is $^5\Delta_g$ with a bond length of 1.98 Å and total magnetic moment of 2 μ_B per Co atom, in good agreement with experiment [33].

3. Results and discussion

3.1. Defect-free $Zn_{1-x}Co_xO$ thin films

We begin with the analysis of the electronic structure and magnetic properties of the (1 × 2) 9-layer $Zn_{0.889}Co_{0.111}O$ thin film supercell. Geometry optimization and total energy calculations were carried out for all the configurations given in figure 1 to study the site preference and distribution of Co atoms in ZnO thin films. Configuration I and configuration II correspond to replacing two Zn atoms with Co at the nearest-neighbor (NN) sites and the farther separated (FS) sites on the surface layer of the slab, respectively. Configuration III is achieved by replacing one Zn on the surface layer and the other on the second layer with Co atoms. Configuration IV and V relate to the substitution of two Zn atoms with two Co atoms at NN sites and FS sites on the second layer, respectively. Configuration VI represents the replacement of NN Zn atoms with Co on the third layer. To preserve the symmetry of the supercell, the corresponding sites on the other side of the slab were respectively replaced with Co atoms for each configuration. The total energies corresponding to both FM and AFM spin alignments between Co atoms were calculated to determine the preferred magnetic ground state. The magnetic coupling is obtained from the total energy difference ΔE between the FM and AFM states ($\Delta E = E_{AFM} - E_{FM}$). Negative ΔE means the AFM state is lower in energy than the FM one. The relative energy $\Delta\varepsilon$ was calculated with respect to the ground state of all the configurations. The calculations for the magnetic moment located at each Co atom

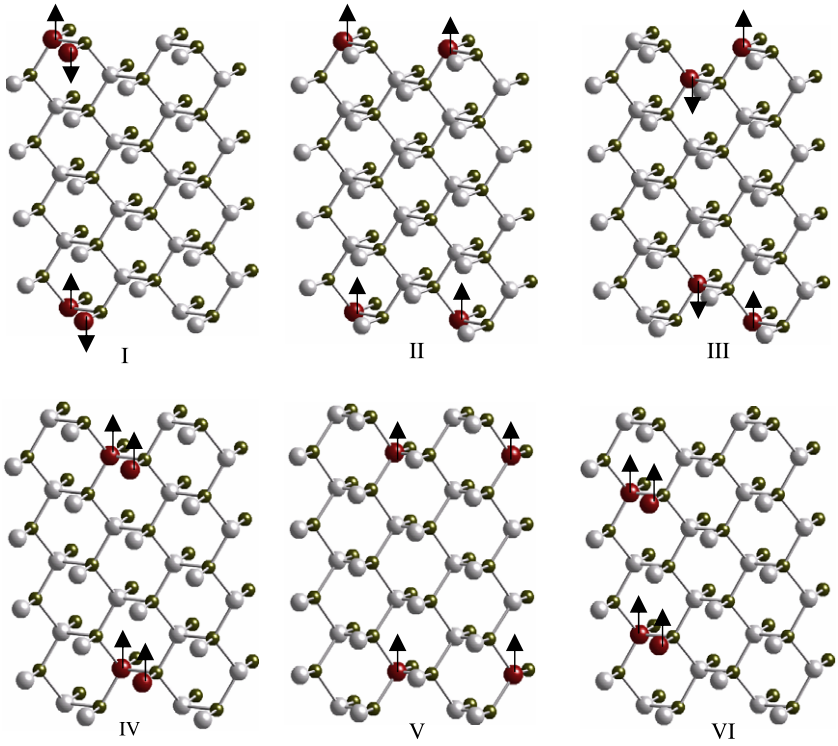

Figure 1. The schematic representation of six configurations of the $Zn_{32}Co_4O_{36}$ thin film supercell. The lighter and bigger spheres are Zn, the darker and smaller spheres are O, and the red and biggest spheres are Co. The arrows show the magnetic coupling between pairs of Co atoms.

Table 1. Energy difference ΔE between AFM and FM states ($\Delta E = E_{AFM} - E_{FM}$, in eV/supercell), relative energy $\Delta\varepsilon$ (in eV) calculated with respect to the ground state configuration I, optimized Co–Co distance $d_{Co1-Co2}$ (in Å), the average Co–O bond length (in Å), and the average magnetic moments (in μ_B) on Co atoms for $Zn_{32}Co_4O_{36}$. The first column specifies the configurations shown in figure 1.

Configurations	ΔE	$\Delta\varepsilon$	$d_{Co1-Co2}$	d_{Co-O}	μ_{Co}
I	−0.465	0.000	2.650	1.837	2.102
II	0.009	0.786	5.628	1.871	1.831
III	−0.184	0.807	2.963	1.916	1.821
IV	0.109	1.280	3.146	1.957	2.503
V	0.008	1.587	5.628	1.976	2.496
VI	0.041	1.450	3.192	1.980	2.511

were also performed self-consistently. The main results are summarized in table 1.

From the relative energies in table 1, we note that configuration I, where two Co atoms are at the NN sites on the surface, is the ground state, while other configurations are higher in energy by 0.786–1.587 eV. This indicates that Co atoms prefer to reside on the surface layer and to be close to each other. This is different from the situation of Mn in ZnO thin films, where Mn exhibits no site preference and, thus, can be distributed uniformly in ZnO thin films [32]. In the ground state configuration, the AFM state is 0.465 eV lower in energy than the FM state. The Co–Co distance and the average Co–O bond length are found to be 2.650 Å and 1.837 Å, respectively, which are significantly shorter than those in the corresponding bulk (3.264 and 1.995 Å, respectively), or those in the bulk-like sites (configuration VI, 3.192 and 1.980 Å, respectively), as a result of surface reconstruction. The total magnetic moment is found to be 0 μ_B, while the moment located on each Co atom is about 2.104 μ_B and mainly comes from the Co 3d orbital (2.075 μ_B), with small contributions arising from Co 4s (0.05 μ_B) and 3p (0.02 μ_B). The two Co atoms are coupled antiferromagnetically. The nearest O atoms are also polarized antiferromagnetically with respect to each of the Co atoms and carry magnetic moments of about 0.015–0.110 μ_B, mainly coming from O 2p orbitals. We also note that the energy difference ΔE dramatically decreases with increasing Co–Co distance. The FM states are about 8–9 meV lower in energy than the AFM states when the two Co atoms are separated by ∼5.6 Å in configuration II and V. The FM and AFM states are almost energetically degenerated. This suggests that the range of magnetic interaction is short in Co-doped ZnO thin films, which is consistent with the calculated results in Co-doped bulk ZnO [26].

We studied the electronic structure of the ground state configuration by calculating the electronic density of states (DOS). These are plotted in figures 2(a_1)–(a_3), where the dotted line indicates the Fermi energy. For comparison we also plotted the total spin DOS for the pure $Zn_{36}O_{36}$ supercell, as shown in figure 2(a). We see that new states are introduced either inside the valence band or above the valence band maximum in the gap region of ZnO when the Co atoms are incorporated. The spin-up and spin-down DOS are totally symmetrical, leading to zero magnetic moment. Thus, the total DOS for the supercell of the $Zn_{0.889}Co_{0.111}O$ thin film clearly shows the AFM feature. The partial DOS for Co and O atoms in figures 2(a_2) and (a_3)

Table 2. Energy difference ΔE between AFM and FM states ($\Delta E = E_{AFM} - E_{FM}$, in eV/supercell), the relative energy $\Delta\varepsilon$ (in eV) calculated with respect to the ground state for each concentration of vacancies, optimized Co–Co distance $d_{Co1-Co2}$ and the average Co–O bond length d_{Co-O} (in Å), and the average magnetic moments (in μ_B) on Co atoms for $Zn_{52}Co_4O_{56}$ with and without defects. The first column specifies the defect configurations, as shown in figure 3, as well as defect concentrations.

Configurations	ΔE	$\Delta\varepsilon$	$d_{Co1-Co2}$	d_{Co-O}	M_{Co}
Without defects	−0.098		2.852	1.864	2.304
C_{Z1} (V_{Zn} at 3.57%)	−0.501	0.000	3.120	1.807	2.385
C_{Z2} (V_{Zn} at 3.57%)	−0.489	1.589	3.034	1.815	2.457
C_{Z3} (V_{Zn} at 3.57%)	−0.951	0.996	2.759	1.802	2.403
C_{11} (V_O at 3.57%)	0.586	0.580	2.270	1.892	2.084
C_{12} (V_O at 3.57%)	−0.034	0.541	2.659	1.862	2.058
C_{13} (V_O at 3.57%)	−0.031	0.000	2.776	1.868	2.269
C_{14} (V_O at 3.57%)	−0.027	1.652	3.108	1.852	2.206
C_{21} (V_O at 7.14%)	0.683	0.875	2.264	1.904	2.071
C_{22} (V_O at 7.14%)	0.668	0.000	2.259	1.898	2.075

show respectively that the majority spin DOS at E_F is mainly composed of Co 3d and O 2p states and there is an overlap between Co 3d and O 2p around the Fermi level.

We then repeated our calculations for the (2 × 2) 7-layer $Zn_{56}O_{56}$ supercell to study the effect of dopant concentration and supercell construction on the magnetic coupling. A Co doping concentration of 7.14% was achieved by substituting two Zn atoms with Co on either side of the slab, which is closer to the concentration studied in most experiments, namely ∼3%–15%. We considered two configurations: one configuration is where two Co atoms substitute Zn at NN sites on the surface layer (similar to C_I in figure 1); another one is constructed by replacing two Zn atoms at FS sites (similar to C_{II} in figure 1). We did not consider configurations where Zn atoms on the subsurface or third layer are replaced by Co since we have demonstrated that Co atoms prefer the surface sites over subsurface or interior sites in ZnO thin films (see table 1). Calculations for the $Zn_{0.928}Co_{0.071}O$ thin film supercell were carried out in the same way as described earlier. We found, once again, that Co atoms like to be close to each other and couple antiferromagnetically. The configuration with Co atoms occupying the NN sites is found to be the ground state with the AFM state being 0.098 eV/supercell lower in energy than the FM state. The Co–Co distance and Co–O bond length are 2.852 and 1.864 Å, respectively. The magnetic moment on each Co atom is about 2.304 μ_B. Another configuration is found to be 0.371 eV higher in energy than the ground state. The main results are summarized in the first row of table 2.

The calculated total spin DOS and the partial spin DOS of Co 3d and O 2p orbitals near the Fermi level for the ground state configuration are plotted in figures 2(b_1)–(b_3), which are quite similar to those for the supercell of the $Zn_{0.889}Co_{0.111}O$ thin film. Namely, the DOSs are characterized by an AFM feature with symmetrical spin-up and spin-down total DOS and new states appearing around the gap region of ZnO (refer to the DOS for the pure ZnO thin film [25]). It was found that the oxidization state of Co is 2+, which is isoelectronic with Zn^{2+}. Thus, no free carriers are introduced due to Co doping. This would be the physical reason for the AFM coupling between Co atoms in $Zn_{1-x}Co_xO$. The same mechanism of carrier-induced ferromagnetism was proposed for $Zn_{1-x}Mn_xO$ thin films [34, 35]. Thus, it is clear that the AFM ordering is energetically favorable, relative to the FM state, and the magnetic coupling between Co atoms is insensitive to the concentration of dopant. This is in agreement with recent experimental observations [12–16], where the $Zn_{1-x}Co_xO$ (x = 0.05–0.15, at%) thin films exhibited AFM or PM behavior. Therefore, that observed FM behavior must be associated with other factors, such as sample preparation conditions or structure defects.

3.2. *Influence of vacancies on the magnetic coupling*

We then investigated the effects of native defects on the magnetic coupling. Several defects or defect complexes can form during the growth of $Zn_xCo_{1-x}O$ thin films. Among them, the most common donor defects are oxygen vacancies (O_V) and Zn interstitials (Zn_i), leading to n-type ZnO. Other defects that could be encountered are zinc vacancies (V_{Zn}) and oxygen interstitials (O_i), resulting in a p-type material. However, depending on preparation conditions, the predominant defects can be Zn interstitials and/or O vacancies (V_O) or Zn vacancies (V_{Zn}). In this study, we concentrated only on V_{Zn} and V_O to shed light on the effect of both p-type and n-type defects on the magnetism of $Zn_xCo_{1-x}O$ thin films.

We first introduced the vacancies in the ground state configuration of the $Zn_{0.89}Co_{0.11}O$ supercell. A V_{Zn} was created by removing a *single* Zn atom nearest to the Co atom on the surface layer of the $Zn_{32}Co_4O_{36}$ slab. To preserve the symmetry, the corresponding Zn atom on the opposite side of the slab was also removed. This led to a $Zn_{30}Co_4O_{36}$ supercell and a V_{Zn} concentration of 5.6%. The geometry optimization and total energy calculations with FM and AFM spin alignments of Co atoms were carried out. It was found that the AFM state is favored over the FM one and the energy difference between the FM and AFM states, ΔE, is decreased from −0.465 to −0.560 eV when the two Zn vacancies are introduced in the system. We then generated O vacancies in $Zn_{32}Co_4O_{36}$ and performed the calculations in the same way. We found, however, that the AFM coupling between Co atoms turns into the FM one with the energy difference ΔE = 0.209 eV/supercell when the O vacancies are closest to Co. In the FM ground state, the distance between the two Co atoms was found to be significantly reduced from 2.650 to 2.290 Å. The large bond length contraction leads to a strong interaction between the Co atoms as well as Co and O atoms, which results in the decrease of magnetic moments on Co atoms, leading to a moment of about 1.908 μ_B on each Co atom and FM coupling between the Co atoms. Thus, our calculated results indicate that V_O is able to stabilize the FM coupling in $Zn_{1-x}Co_xO$, while V_{Zn} favors AFM coupling.

To further verify the onset of ferromagnetism due to V_O and to study the effect of vacancy distribution and concentration on the magnetic coupling, we have created vacancies at different sites in the 2 × 2 7-layer $Zn_{56}O_{56}$ supercell, which has twice the number of Zn–O dimers and allows many more possible sites for introducing vacancies.

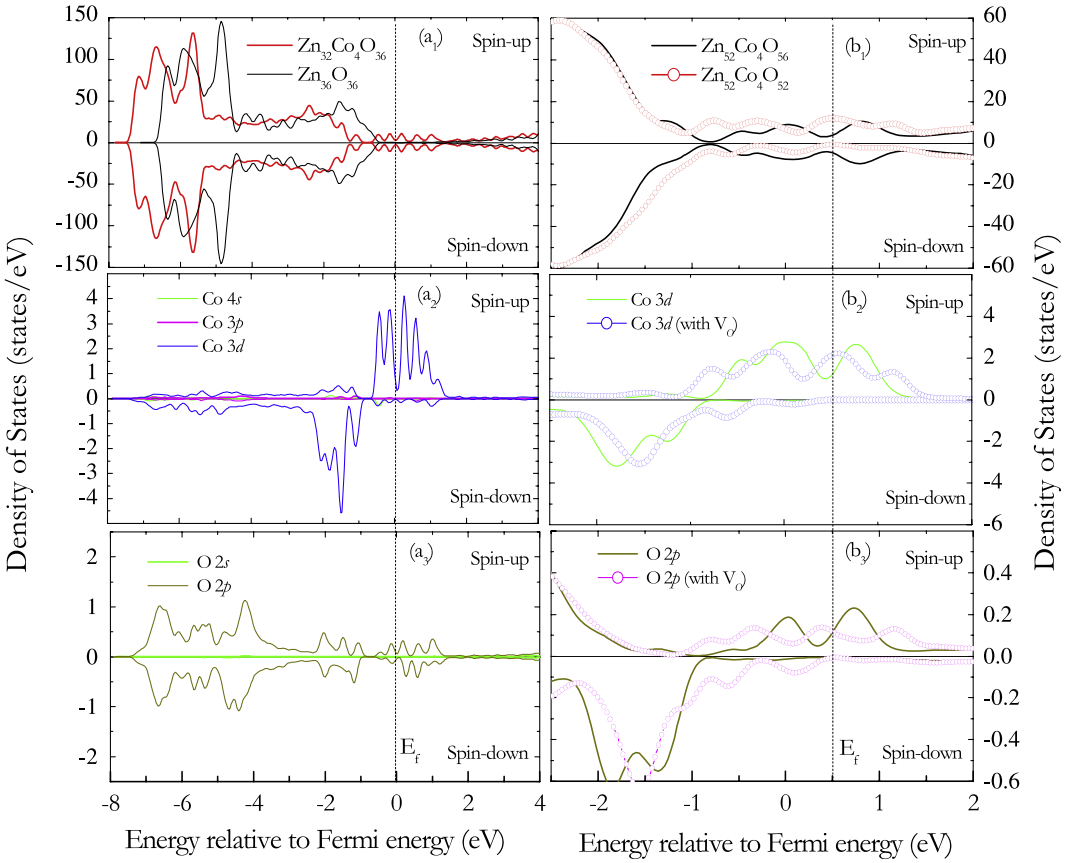

Figure 2. (a_1)–(a_3) Total spin DOS, partial spin DOS of Co and O atoms corresponding to the $Zn_{32}Co_4O_{36}$ supercell. (b_1)–(b_3) Total spin DOS, partial spin DOS of Co 3d and O 2p orbitals corresponding to the $Zn_{52}Co_4O_{56}$ supercell with and without the oxygen vacancies.

We started with the ground state configuration of $Zn_{52}Co_4O_{56}$ and created Zn vacancies at different sites on the surface and subsurface layers of the slab (see configurations C_{Z1}, C_{Z2}, and C_{Z3} in figure 3). O vacancies at different sites, corresponding to configuration C_{11} to C_{22}, were then generated, as shown in figure 3. We studied the energetics of FM and AFM coupling between Co atoms for all these configurations, following the same procedure as described above for the $Zn_{0.89}Co_{0.11}O$ supercell. The calculated results are given in table 2.

The calculated results clearly show that Zn vacancies stabilize the AFM coupling and lead to a strong AFM interaction between the two Co ions. The energy difference ΔE between the FM and AFM states changed from -0.098 to -0.501, -0.489 and -0.951 eV respectively for configurations C_{Z1}, C_{Z2}, and C_{Z3}. From the relative energy, we note that it costs less energy to generate a V_{Zn} close to a Co atom. When O vacancies are generated, on the other hand, the energy difference ΔE is considerably increased. For instance, the AFM coupling turns into the FM one with a large energy difference $\Delta E = 0.586$ eV/supercell in configuration C_{11}. For other configurations C_{12} to C_{14}, ΔE increases from -0.098 eV to -0.034, -0.031 and -0.027 eV, respectively. The ground state configuration was found to be configuration C_{13}, which is still AFM, indicating that it is easer to create a V_O further from Co atom. We, therefore, realized that a small concentration of V_O cannot lead to a transition from AFM to FM states, as confirmed by experiments [20].

It is interesting to see that the FM state becomes much more stable than the AFM state for both configurations C_{21} and C_{22} in figure 3 when the V_O concentration is increased to 7.14% by removing two O atoms on either side of the slab. The energy difference, ΔE, is 0.683 and 0.668 eV/supercell for C_{21} and C_{22}, respectively. This indicates that V_O is capable of tuning the magnetic coupling between Co atoms and stabilizing ferromagnetism in Co-doped ZnO when the concentration of V_O reaches a certain value. We note that configuration C_{22} is lower in energy by 0.875 eV than configuration C_{21}, demonstrating that V_O prefers to distribute uniformly in ZnO thin films. However, for Mn-doped ZnO, there is a reverse correlation: V_{Zn} or nitrogen replacing oxygen is the defect that is responsible for ferromagnetism [35].

The calculated total spin DOS, the partial DOS of Co 3d and O 2p for the ground state of configuration C_{22} are plotted in figures 2(b_1)–(b_3), respectively. We see a significant change of the DOS around the Fermi level when O vacancies are introduced. The total DOS for spin-up and spin-down are no longer identical, indicating that there is a moment in the system. The Fermi level with V_O present slightly moves to a higher energy range compared to that for $Zn_{52}Co_4O_{56}$. The main effect of V_O on the DOS, shown in figure 2(b_2), is a downward shift of the Co 3d spin-up states and an upward shift of the spin-down states, and there is a new peak appearing at 1.24 eV above the Fermi level in the spin-up DOS. These show that the O vacancies have introduced new

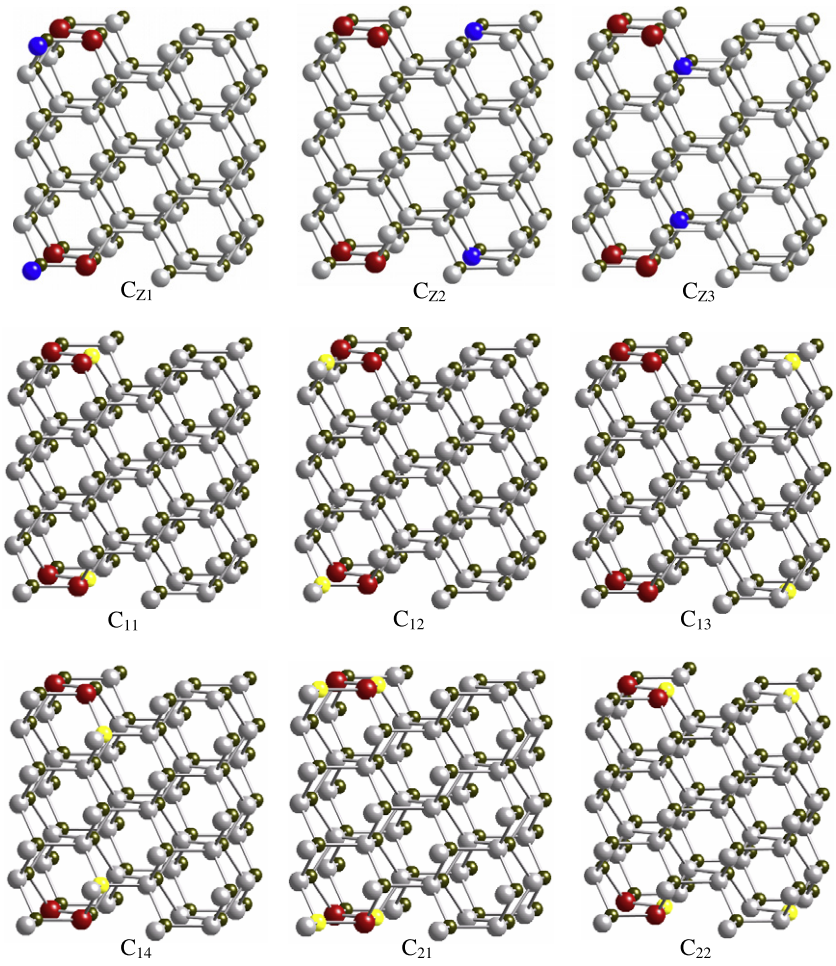

Figure 3. The schematic representation of the nonequivalent vacancy configurations in the ground state of the $Zn_{52}Co_4O_{56}$ supercell. The lighter (bigger) spheres represent the Zn atoms, the darker (smaller) spheres represent the O atoms, and the red (biggest) spheres represent Co atoms. The blue (dark medium sized) and yellow (grey medium sized) spheres specify the sites where the atoms are removed to generate Zn and O vacancies, respectively.

states in the gap region, resulting in FM coupling. This is due to the fact that Co atoms in $Zn_{1-x}Co_xO$ thin films behave as Co^{2+} (d^5). The Co^{2+} can readily substitute the group II cation, Zn, without the formation of structural defects or the generation of carriers, while when a V_O is generated, two more electron carriers are introduced to the system. O vacancies which are known as shallow level donors can supply s, p spin carriers, and doped Co can supply local moments (spins). The s, p electrons partially delocalize onto Co^{2+} and couple to the local spins *via* a FM s, p–d exchange interaction. The Zeeman splitting of the hopping s, p carriers in a modest field can be comparable to the thermal energy (k_BT), which gives rise to the new states of Co 3d and, consequently, to the FM coupling in the n-type Co^{2+}:ZnO thin films. Our finding is consistent with the previous theoretical prediction that sufficient electron carriers are required to achieve ferromagnetism in *bulk* $Zn_{1-x}Co_xO$ [26], and is supported by the recent experiments where oxygen vacancies are found to make ZnO:Co ferromagnetic [20–22]. It has been found in experiment [22] that magnetism changes with the concentrations of Co and vacancies in Co-doped ZnO. Oxygen vacancies can be introduced by vacuum annealing, when the vacancy concentration is enough to give an effective polaron radius of 7.8 Å, and when the Co concentration reaches 1.2%, the system displays strong ferromagnetism. The concentration of oxygen vacancies in the ZnO lattice can also be controlled by changing the oxygen concentration during the sample preparation [20]. Currently there is no report on the direct measurement of oxygen vacancy concentration in Co-doped ZnO.

4. Conclusions

In summary, using spin polarized DFT with GGA and the slab models, we systematically studied the magnetic coupling between Co ions in ZnO thin films. We show that: (1) in contrast to Mn-doped ZnO thin films where Mn atoms are homogeneously distributed, Co ions prefer to cluster and reside on the surface of ZnO thin films; (2) when Co is substitutionally doped in ZnO, Co^{2+} ions replace Zn^{2+} without introducing any carriers, and the magnetic coupling between Co ions is intrinsically AFM. (3) The coupling changes from AFM to FM when the concentration of V_O reaches a certain critical value. The interaction between the localized spins on the Co ions and delocalized carriers–electrons originating from

the O vacancies is responsible for the magnetic transition. (4) Instead of clustering, V_O distributes homogeneously on the surface of $Zn_{1-x}Co_xO$ thin films. (5) V_{Zn}, however, likes to be close to the dopants and makes the system more AFM. Therefore, the observed magnetic properties strongly depend on the experimental conditions and hence are the root cause of the experimental controversy.

Acknowledgments

The work was supported in part by a grant from the Department of Energy and from the National Science Foundation of China (NSFC-10744006 and NSFC-10874007).

References

[1] Dietl T, Ohno H, Matsukura F, Cibert J and Ferrant D 2000 *Science* **287** 1019
[2] Jayaram V, Rajkumar J and Sirisha Rani B 1999 *J. Am. Ceram. Soc.* **82** 473
[3] Ueda K, Tabata H and Kawai T 2001 *Appl. Phys. Lett.* **79** 988
[4] Lee H-J, Jeong S-Y, Cho C R and Park C H 2002 *Appl. Phys. Lett.* **81** 4020
[5] Prellier W, Fouchet A, Mercey B, Simon Ch and Raveau B 2003 *Appl. Phys. Lett.* **82** 3490
[6] Venkatesan M, Fitzgerald C B, Lunney J G and Coey J M D 2004 *Phys. Rev. Lett.* **93** 177206
[7] Yang J H, Cheng Y, Liu Y, Ding X, Wang Y X, Zhang Y J and Liu H L 2009 *Solid State Commun.* **149** 1164
[8] Jin Z, Fukumura T, Kawasaki M, Ando K, Saito H, Sekiguchi T, Yoo Y Z, Murakami M, Matsumoto Y, Hasegawa T and Koinuma H 2001 *Appl. Phys. Lett.* **78** 3824
[9] Lawes G, Risbud A S, Ramirez A P and Seshadri R 2005 *Phys. Rev.* B **72** 165202
[10] Yin S, Xu M X, Yang L, Liu J F, Rösner H, Hahn H, Gleiter H, Schild D, Doyle S, Liu T, Hu T D, Takayama-Muromachi E and Jiang J Z 2006 *Phys. Rev.* B **73** 224408
[11] Ney A, Ollefs K, Ye S, Kammermeier T, Ney V, Kaspar T C, Chambers S A, Wilhelm F and Rogalev A 2008 *Phys. Rev. Lett.* **100** 157201
[12] Shi T, Zhu S, Sun Z, Wei S and Liu W 2007 *Appl. Phys. Lett.* **90** 102108
[13] Xu Q Y, Zhou S, Marko M, Potzger K, Fassbender J, Vinnichenko M, Helm M, Hochmuth H, Lorenz M, Grundmann M and Schmidt H 2009 *J. Phys. D: Appl. Phys.* **42** 085001
[14] Ando K, Saito H, Jin Z W, Fukumura T, Kawasaki M, Matsumoto Y and Koinuma H 2001 *Appl. Phys. Lett.* **78** 2700
[15] Bouloudenine M, Viart N, Colis S, Kortus J and Dinia A 2005 *Appl. Phys. Lett.* **87** 052501
[16] Sati P, Deparis C, Morhain C, Schäfer S and Stepanov A 2007 *Phys. Rev. Lett.* **98** 137204
[17] Kittilstved K R, Schwartz D A, Tuan A C, Heald S M, Chambers S A and Gamelin D R 2006 *Phys. Rev. Lett.* **97** 037203
[18] Schwartz D A and Gamelin D R 2004 *Adv. Mater.* **16** 2115
[19] MacManus-Driscoll J L, Khare N, Liu Y L and Vickers M E 2007 *Adv. Mater.* **19** 2925
[20] Biegger E, Fonin M, Rüdiger U, Janßen N, Beyer M, Thomay T, Bratschitsch R and Dedkov Y S 2007 *J. Appl. Phys.* **101** 073904
[21] Gacic M, Jakob G, Herbort C, Adrian H, Tietze T, Brück S and Goering E 2007 *Phys. Rev.* B **75** 205206
[22] Sudakar C, Kharel P, Lawes G, Suryanarayanan R, Naik R and Naik V M 2007 *J. Phys.: Condens. Matter* **19** 026212
[23] Zhang S B, Wei S-H and Zunger A 2001 *Phys. Rev.* B **63** 075205
[24] Janotti A and Van de Walle C G 2007 *Phys. Rev.* B **76** 165202
[25] Wang Q, Sun Q, Chen G, Kawazoe Y and Jena P 2008 *Phys. Rev.* B **77** 205411
[26] Lee E-C and Chang K J 2004 *Phys. Rev.* B **69** 085205
[27] Spaldin N A 2004 *Phys. Rev.* B **69** 125201
[28] Wang Y and Perdew J P 1991 *Phys. Rev.* B **44** 13298
[29] Kresse G and Joubert J 1999 *Phys. Rev.* B **59** 1758
[30] Kresse G and Furthmüller J 1996 *Phys. Rev.* B **54** 11169
[31] Monkhorst H J and Pack J D 1976 *Phys. Rev.* B **13** 5188
[32] Wang Q and Jena P 2004 *Appl. Phys. Lett.* **84** 4170
[33] Yanagisawa S, Tsuneda T and Hirao K 2000 *J. Chem. Phys.* **112** 545
[34] Sato K and Yoshida H K 2002 *Semicond. Sci. Technol.* **17** 367
[35] Wang Q, Sun Q, Jena P and Kawazoe Y 2004 *Phys. Rev.* B **70** 052408